

Structural, Morphological and Optical Parameters of Zn(1-x)Cu_xS Thin Films for Optoelectronic Devices

A. Almohammed¹, A. Ashour^{1,2} and E. R. Shaaban^{3,*}

¹Physics Department, Faculty of Science, Islamic University, P. O. Box 170, Al Madinah, Saudi Arabia

²Physics Department, Faculty of Science, Minia University, El Minia, Egypt

³Physics Department, Faculty of Science, Al-Azhar University, Assuit, 71542, Egypt

Received: 13 Oct. 2021, Revised: 22 Dec. 2021, Accepted: 15 Jan. 2022

Published online: 1 May 2022

Abstract: In the present work, ZnS and Cu incorporated at (2%, 4%, 6%, 8%, and 10%) thin films were growth onto hot glass substrates at substrates temperature 270 °C with thickness about 100 nm by chemical spray pyrolysis technique. The solutions of the spray consists of Zn(CH₃COO)₂·2H₂O, SC(NH₂)₂ and CuCl₂·2H₂O with molar concentration 0.1M/L. The structure of the film was studied by XRD pattern, the results shows that the films were polycrystalline with cubic phase for pure ZnS and hexagonal phase for Zn_{1-x}Cu_xS at x=10%. The optical constants, refractive index, *n* and extinction coefficient, *k* were determined The optical energy gap of the direct transition is also estimated, pure ZnS is 3.42 eV, and it increases as the Cu concentration increases from 3.49 to 3.67 eV. The room temperature photoluminescence (PL) of copper-doped zinc sulfide (ZnS:Cu) nanoparticles was studied. Through Gaussian fitting, the PL spectrum of undoped ZnS nanoparticles is deconvoluted into two blue luminescence peaks (centered at 411 nm and 455 nm, respectively), both of which can be attributed to the recombination of ZnS defect states. But for doped samples, a third peak at about 500 nm was also identified. Discussed the changes of all optical constants and PL spectra from the changes of optoelectronics microstructure parameters

Keywords: Zn_{1-x}Cu_xS pyrolysis technique; thin film; microstructural parameters; optical constants; photoluminescence.

1 Introduction

In recent years, much effort has been devoted to the research of doped metal chalcogenide nanostructured materials. This type of nanomaterials exhibits unusual physical and chemical properties in comparison with their bulk materials, such as size-dependent variation of the band gap energy [1, 2]. The ZnS bulk form has a direct-wide bandgap (3.66 eV), good visible region transparency, excellent transport properties and good thermal stability [3]. These characteristics make ZnS widely used in various applications in the electronics industry, such as ultraviolet light emitting diodes, solar selective decorative coatings, lasers, optoelectronic and electroluminescent devices [4-7]. ZnS can take one of two crystallographic phases, the combination of cubic zinc blend structure or hexagonal wurtzite structures [8, 9]. The position of chalcogenide semiconductor materials in the luminescence band is affected by the dopant type (Mn²⁺, Cu²⁺, Cr³⁺ and Ni²⁺) and their concentrations in the matrix [10]. Inside the band gap,

the dopants induced a number of impurity states that can normally reduce the material's energy barrier [11]; dopants or impurities create discrete energy levels that can improve the material's electronic, optical, and magnetic performance [12]. Visible-light absorption and photocatalytic hydrogen production activity are enhanced as copper replaces zinc in ZnS (wurtzite) [13]. Due to the hybridization between the d and p states of Cu and S atoms, the energy gap of Zn_{1-x}Cu_xS was reduced [14]. In addition, the ZnS photoluminescence spectrum: 1% Cu/Polyvinyl Alcohol (PVA) nanocomposite film showed higher photoluminescence intensity compared to other Cu nanocomposite films doped from ZnS / PVA [15]. All of the above and other properties nominate the copper-doped ZnS system to be used in many applications, such as LEDs, X-ray screens, and optical lasers [16]. The thin films of ZnS are usually prepared by different techniques such as sputtering, chemical bath, MOCVD techniques, vacuum evaporation, flash evaporation and spray pyrolysis [17, 18]. Spray pyrolysis is a simple inexpensive method especially for substances which have water soluble salts. So we have used this method to obtain ZnS thin films on glass substrate. The objectives of this paper are to study the effect of copper content on the microstructure, optical

*Corresponding author E-mail: esam_ramadan2008@yahoo.com

parameters and photo luminescence of ZnS films for photoelectronic applications.

2 Materials and Methods

Pure and doped ZnS thin films were prepared on glass substrates. The spraying solution can be prepared by solving zinc acetate [$\text{Zn}(\text{CH}_3\text{COO})_2$](1.097g), thiourea [$\text{SC}(\text{NH}_2)_2$](0.3805 g) & copper chloride [$\text{CuCl}_2 \cdot 2\text{H}_2\text{O}$](0.852 g) in the distilled water to prepared solution with molarities (0.1). The substrate temperature at 270 °C was controlled using the Ni (NiCr thermocouples) thermocouple. The content of Cu in the $\text{Zn}_{1-x}\text{Cu}_x\text{S}$ films are controlled by fixing all the weights of the dissolved materials and fixing the procedure of reaction process as mentioned in the preparation method of the solution. The authors used molecular weights calculations to change the atomic content of Cu in the $\text{Zn}_{1-x}\text{Cu}_x\text{S}$ films. The deposition time for one layer being about 2 sec. The spraying process was done in the absence of air flow. The thickness of the film is measured by spectroscopic ellipsometry technique. After 20 minutes (about 600 layers), the thickness of all prepared films varied between 100-110 nm. The elemental composition of the films was analyzed by using energy dispersive X-ray spectrometer unit (EDAX) interfaced with a scanning electron microscope, SEM (JEOL JSM-6360LA, Japan) operating an accelerating voltage of 30 kV, which was used to study the morphology of the film. The structure of the prepared samples was analyzed by XRD analysis (Philips X-ray diffractometry (1710)) with Ni-filtered $\text{Cu K}\alpha$ radiation with $\lambda = 0.15418$ nm). Using a computer-controlled spectrophotometer with dual beams (Shimadzu UV-2101 combined with PC), transmittance and reflectance measurements are performed in the wavelength range of 300 to 2500 nm under normal light incident conditions. Room temperature photoluminescence (PL) Using a Jobin Yvon H25 fluorescence spectrophotometer with a 325 nm He-Cd laser line as the excitation source, the powder samples were measured to characterize the luminescence characteristics of the nanoparticles.

3 Results and Discussion

3.1 Structural Analysis

The typical EDAX spectra of ZnS and $\text{Zn}_{0.94}\text{Cu}_{0.06}\text{S}$ and $\text{Zn}_{0.90}\text{Cu}_{0.10}\text{S}$ films are shown in Figure 1 (a, b, and c), respectively. The observed peaks indicate the stoichiometric composition of Cd, S, and Cu. The typical EDAX spectra of ZnS, $\text{Zn}_{0.94}\text{Cu}_{0.06}\text{S}$ and $\text{Zn}_{0.90}\text{Cu}_{0.10}\text{S}$ films are shown in Figure 1 (a, b, and c), respectively. The observed peaks indicate the

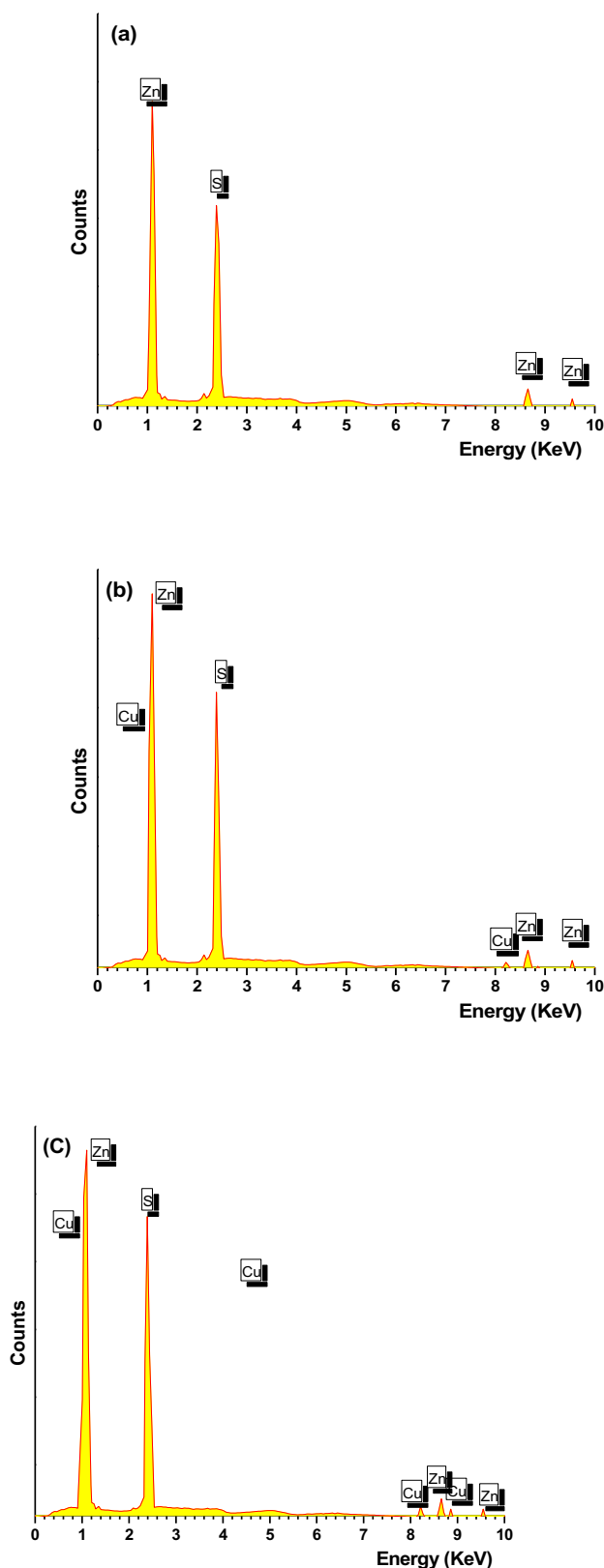


Fig. 1: EDAX spectra for (a) ZnS, (b) $\text{Zn}_{0.96}\text{Cu}_{0.04}\text{S}$, and (c) $\text{Zn}_{0.90}\text{Cu}_{0.10}\text{S}$ thin films.

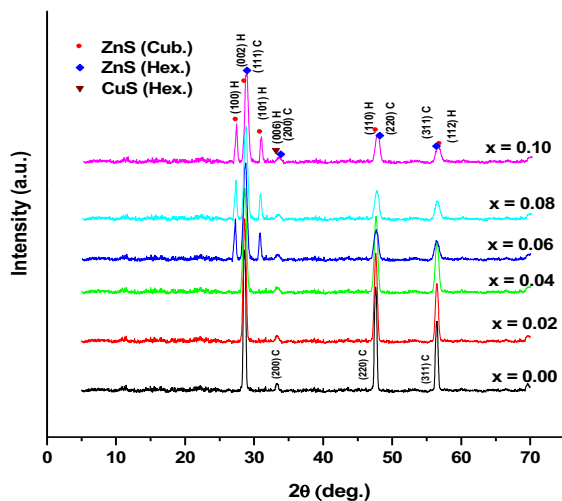


Fig. 2: XRD patterns of Zn_{1-x}Cu_xS thin films.

stoichiometric composition of Cd, S and Cu. It can be seen that in the CdS_{1-x}Cu_x system, the content of Cu increases with the increase of Cu concentration; this indicates that Cu²⁺ ions have successfully included the acceptor into the ZnS lattice. These results are very consistent with the experimental composition used in the current system.

The X-ray diffraction pattern of the obtained Zn_{1-x}Cu_xS ($x = 0.0, 0.02, 0.04, 0.06, 0.08, 0.10$) sample is shown in Figure 2. The 0.0, 0.02, and 0.04 XRD patterns are similar to a single phase without other phases or oxides with a cubic zinc mixture structure. For films with $x = 0.6, 0.08,$ and 0.10 and a high percentage of copper ions in ZnS, the XRD pattern shows a polycrystalline structure and a mixture of cubic and hexagonal ZnS and a small amount of copper sulfide (CuS) secondary phase according to the American taste material Standard (ASTM) card [JCPDS-ICDD document No. 96-500-0089 for cubic ZnS, No. 96-101-1197 for hexagonal ZnS and No. 96, -900- is observed at ($x = 0.10$) 0524 is used for CuS]. As the Cu concentration increases, the strength of the Zn_{1-x}Cu_xS film decreases.

The thin film scanning electron microscope images (SEM) of ZnS, Zn_{0.96}Cu_{0.04}S and Zn_{0.90}Cu_{0.10}S are shown in Figure 3 (a, b, and C). It is found that the density of thin film ZnS is lower than that of thin film ZnS:Cu. However, as the Cu dopant concentration increases, a denser ZnS:Cu film can be obtained. The value of average grain size increases significantly with the increase of Cu content [24]. El-Sayed et al. [25] This phenomenon has also been observed in Cu-doped ZnO films grown on glass substrates using the sol-gel method.

3.2 Optical Characterization

3.2.1 Refractive Index and Optical Band Gap

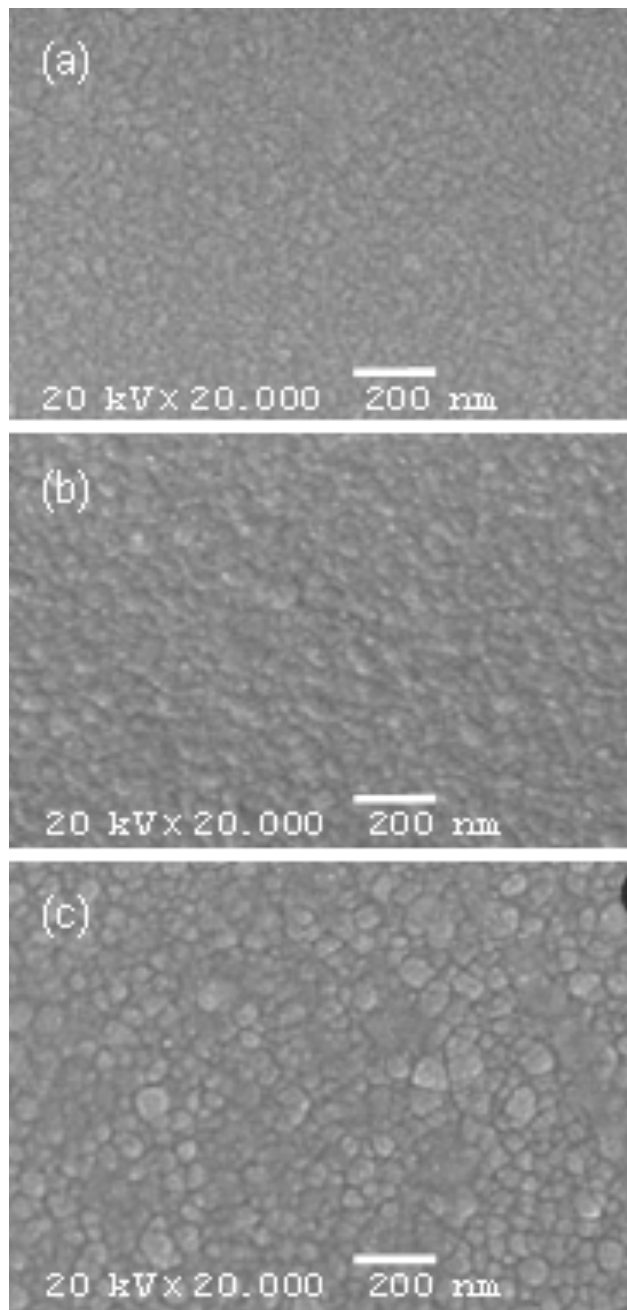


Fig. 3: Scanning electron microscope images (SEM) of (a) ZnS, (b) Zn_{0.96}Cu_{0.04}S, (c) Zn_{0.90}Cu_{0.10}S thin films.

The optical transmittance, $T(\lambda)$ and reflectance, $R(\lambda)$ spectrum of UV-VIS-NIR of Zn_{1-x}Cu_xS ($x = 0, 0.02, 0.04, 0.06, 0.08,$ and 0.10 at. %) of the as deposited films are shown in Fig. 5. One can see that the transmittance is generally increased with increased wavelength and in the visible region there is transparency. Additionally, the smoothing of the transmission spectrum confirmed excellent quality and homogeneity for these Cu doped ZnS thin films [19, 20]. The transmission spectrum in the VIS-NIR regions

varies from about 0.857 for the first film (with $x = 0$ at. %) to 0.789 for the last film (with $x = 0.10$ at. %). The high transmittance properties in the VIS-NIR regions allow for the use of thin films in modern applications such as thermal control of window coatings and also for anti-reflective coatings. On the other hand, reflectance rises significantly from 0.13 (with $x = 0$ at.%) to roughly 0.17 in the VIS-NIR regions (with $x = 0.10$ %). The refractive index (n) is also an important parameter for practical applications relating to the electronic polarization of the ions as the electrical field within the material wall.

The refractive index (n) of the examined thin films was determined using only the experimentally measured transmission data [26-28], based on the envelope method proposed by Swanepoel, more details about the Swanepoel's method in reference [26-28].

Based on envelop method the index of refraction n can be determined at any wavelength utilizing the next formula [26-28]:

$$n(\lambda) = 2S_s \left[\frac{(T_M - T_m)}{(T_M T_m)} \right] + \left[\frac{S^2 + 1}{2} \right] + \sqrt{ \left\{ 2S_s \left[\frac{(T_M - T_m)}{(T_M T_m)} \right] + \left[\frac{S^2 + 1}{2} \right] \right\}^2 - S^2 } \quad (2)$$

where S is the index of refraction of the substrate, which can be determined in terms of transmission of substrate. T_s from the relationship [29]:

$$s(\lambda) = (T_s(\lambda))^{-1} + \sqrt{((T_s(\lambda))^{-2} - 1)} \quad (3)$$

and the $T_s(\lambda)$ at any wavelength can be determined in terms of the polynomial fitting of third order as follows:

$$T_s(\lambda) = 0.8914 - 8.024 \times 10^{-5} \lambda + 6.138 \times 10^{-8} \lambda^2 - 1.38877 \times 10^{-11} \lambda^3$$

Fig.7 shows the dependence of the refractive index, n of $Zn_{1-x}Cu_xS$ ($x = 0, 0.02, 0.04, 0.06, 0.08, \text{ and } 0.10$ at. percent) films on wavelength. It is obvious that n is reduced for all films with an increase of λ and it increases with an increase in concentration of Cu. The explanation for this behavior may be due to an increase in the number of atoms at interstitial locations, resulting in impurity form dispersing centers in the films under investigation [30, 31]. Now, to get the refractive index-wave length dependence over the whole spectral range, the well-known two-term Cauchy function, $n(\lambda) = B + A/\lambda^2$ can be used. According to this function, refractive index n can be fitted, see Fig. 4. The resultant values of Cauchy coefficients, A and B are shown in the inset of Fig. 5.

The absorption coefficient, on the other hand, is defined as a measure of the percentage of loss in light directly at a given thickness from the falling beam. The absorption coefficient, $\alpha(\lambda)$ can be calculated in a strong absorption region using the spectra of $T(\lambda)$ and $R(\lambda)$ [32, 33] as follows:

$$\alpha(\lambda) = \frac{1}{d} \times \ln \left[\frac{(1-R(\lambda))^2 + \sqrt{\{(1-R(\lambda))^4 + 4(R(\lambda)T(\lambda))^2\}}}{2T(\lambda)} \right] \quad (4)$$

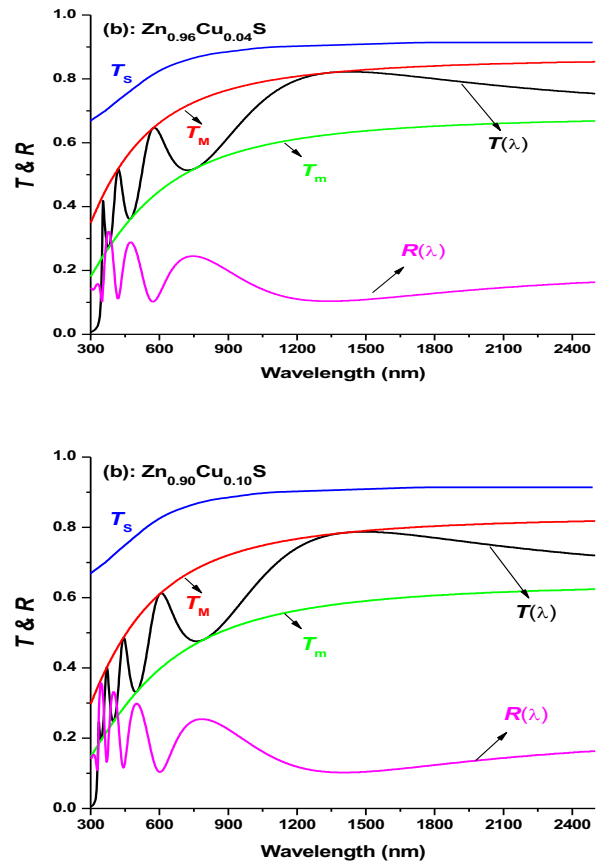


Fig. 4: The optical transmittance $T(\lambda)$ dependence of wavelength λ for (a) ZnS, (b) $Zn_{0.96}Cu_{0.04}S$, (c) $Zn_{0.90}Cu_{0.10}S$ thin films with the T_s , T_{Max} and T_{min} .

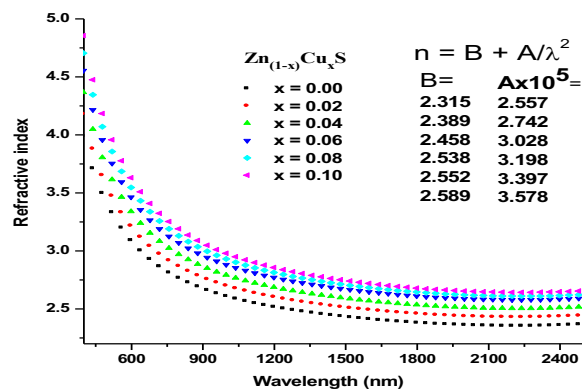


Fig. 5: The refractive index n with wavelength λ of $Zn_{(1-x)}Cu_xS$ thin films. The inset is a Cauchy coefficient.

Where the film thickness is d (cm). Fig. 6 illuminates the α vs $h\nu$ for the $Zn_{1-x}Cu_xS$ films. One can see that with increased concentration of Cu the value α increases. The optical energy band can be calculated using the values of the absorption coefficient (α) according to the following formula [29] in order to verify the optical transition nature of $Zn_{1-x}Cu_xS$ as-deposited thin films.

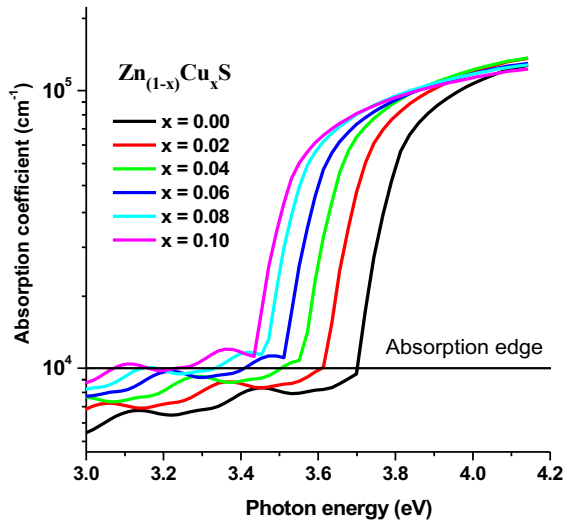


Fig. 6: The absorption coefficient α with the photon energy $h\nu$ for $Zn_{(1-x)}Cu_xS$ thin films.

$$\alpha(h\nu) = \frac{K(h\nu - E_g^{opt})^m}{h\nu} \quad (5)$$

Where K is an independent parameter for the individual transitions [34], E_g^{opt} is the optical energy gap and m is a number identifying the transition type. Different authors [35-37] recommended different m values, such as $m = 2$ for the majority of amorphous semiconductors (indirect transition) and $m = 1/2$ for most crystalline semiconductors (direct transition). The direct transition is valid for different film of $Zn_{1-x}Cu_xS$. Figure 7 illustrates the best fit of $(\alpha h\nu)^2$ vs. $h\nu$ for varying concentration of Cu on $Zn_{1-x}Cu_xS$ films.

The direct optical band gap may be taken as the of $(\alpha h\nu)^2$ against $(h\nu)$ at $(\alpha h\nu)^2 = 0$. For each film the result is shown in Fig. 10. The E_g^{opt} reduces as Cu concentration increases in $Zn_{1-x}Cu_xS$ film. Possibly the decrease in the value of E_g^{opt} can be due to the inclusion of Cu ions in the lattice, which results in the bandgap acceptor levels. In II-VI materials the acceptor rates fall and join the valence band which causes the valence band to expand into the prohibited region which reduces the bandgap, related trend has been illustrated [38-40]. Also, this decrease in E_g^{opt} with Cu dopant can be attributed to the increase in pores and the

compositional modifications, which can result in lower density and polarizability. The observed E_g^{opt} results are well consistent with preceding studies [41, 42].

The extinction coefficient (k) of the $Zn_{1-x}Cu_xS$ films were evaluated from the absorption and using the relationship $\alpha = 4\pi k/\lambda$, where λ is wavelength and α is absorption coefficient. The influence of the ZnS thin film Cu dopant on the k can be seen in Fig. 8. It's obvious that the k increases with the Cu content increasing.

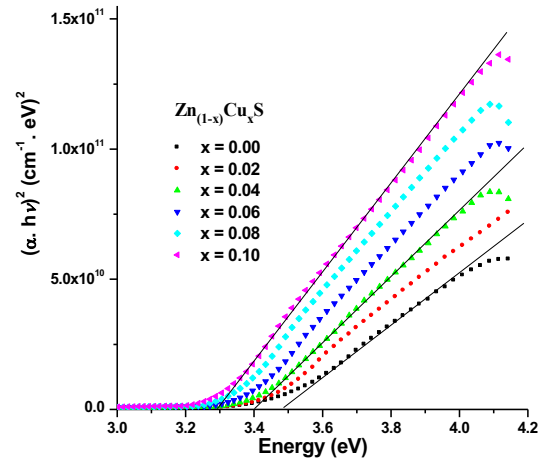


Fig. 7: $(\alpha h\nu)^2$ vs. photon energy $h\nu$ for $Zn_{(1-x)}Cu_xS$ thin films.

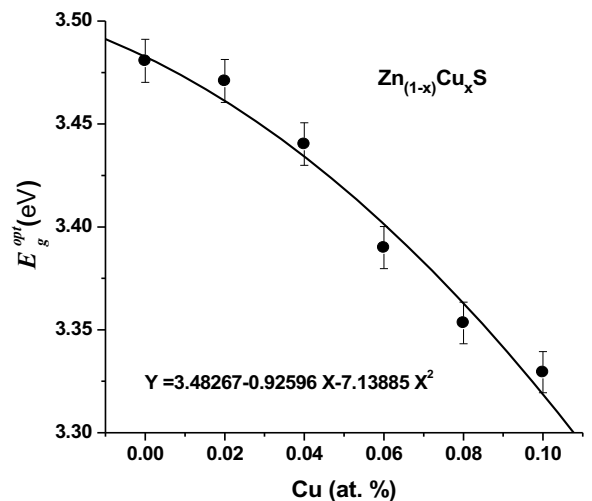


Fig. 8: The band gap E_g^{opt} as a function of Cu content.

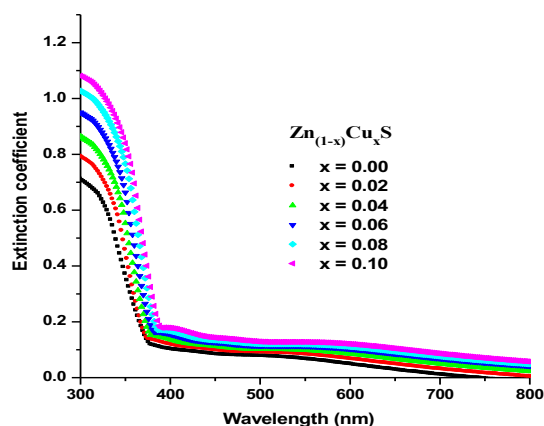


Fig. 9: The Exinction coefficient, k with wavelength λ of $\text{Zn}_{(1-x)}\text{Cu}_x\text{S}$ thin films.

4 Conclusions

In this study, ZnS and Cu incorporated at (0.02, 0.04, 0.06, 0.08, and 0.10 at. %) thin films were growth onto hot glass substrates at substrates temperature 275 °C with thickness about 110 nm by chemical spray pyrolysis technique. EDAX spectra indicate that the Cu^{2+} ions have successfully included acceptor into the ZnS lattice. The obtained X-ray diffraction patterns for $\text{Zn}_{1-x}\text{Cu}_x\text{S}$ indicated for $x = 0.0, 0.02$ and 0.04 a single phase with no other phases or oxides having a cubic zinc blend structure. But for films for $x = 0.6, 0.08$ and 0.10 with a higher percentage of copper ions in ZnS, the XRD pattern shows a polycrystalline structure and a mixture of cubic and hexagonal phases for ZnS and a small traces of copper sulphide (CuS) phase. Using the method of envelop for transmission spectra using fitting exponential of first order for both T_M and T_m , the refractive index of films was calculated. The optical band gaps for the direct transition were estimate and it was 3.44 eV for pure ZnS and decreased with increasing Cu concentration from 3.44 to 3.32 eV. All these The changes of all optical parameters were discussed in terms of microstructure parameters for optoelectronic applications.

Acknowledgment

The authors thank the Deanship of Scientific Research at Islamic University, Al Madinah, Saudi Arabia for funding this research via the 11th (Takamul) program of Academic year 1441 – 1442 AH, research project No. (123). In addition, the authors are grateful to Al-Azhar University (Assiut branch) for supporting with the experimental measurements.

Conflict of Interest

All authors declare that there is no conflict of interest regarding the publication of this paper.

References

- [1] B. Barrocas, T.J. Entradas, C.D. Nunes, O.C. Monteiro, Appl. Catal. B Environ. 218, 709 (2017).
- [2] M.C. Wong, L. Chen, G. Bai, L.B. Huang, J.H. Hao, Adv. Mater., **29**, 1701945 (2017)
- [3] A.F. Al-Hossainy, M.S. Zoromba, J. Alloy. Compd. 789, 670 (2019).
- [4] A.F. Al-Hossainy, M.R. Eid, MSh. Zoromba, J. Electron. Mater., **48(12)**, 8107 (2019).
- [5] M.S. Zoromba, M. Bassyouni, M.H. Abdel-Aziz, A.F. Al-Hossainy, N. Salah, A.A. Al-Ghamdi, M.R. Eid, Appl. Phys., **A 125(9)**, 642 (2019).
- [6] A.F. Al-Hossainy, A. Ibrahim, M.S. Zoromba, J. Mater. Sci. Mater. Electron. 30(12), 11627 (2019).
- [7] M.H. Abdel-Aziz, A.F. Al-Hossainy, A. Ibrahim, S.A. Abd El-Maksoud, M. Sh. Zoromba, M. Bassyouni, S.M.S. Abdel-Hamid, A.A.I. Abd-Elmageed, I.A. Elsayed, O.M. Alqahtani, J. Mater. Sci. Mater. Electron., **29(19)**, 16702 (2018)
- [8] G.C. Trigunyat, G.K. Chanda, Phys. Status Solidi A., **4**, 9 (1971)
- [9] G. Murugadoss, B. Rajamannan, V. Ramasamy, J. Lumin., 130, 2032 (2010)
- [10] P. Liao, E.A. Carter, Chem. Soc. Rev., **42**, 2401 (2013)
- [11] A.L. Curcio, L.F. da Silva, M.I.B. Bernardi, E. Longo, A. Mesquita, J. Lumin., **206**, 292 (2019).
- [12] S. Prasanth, P. Irshad, D.R. Raj, T.V. Vineeshkumar, R. Philip, C. Sudarsanakumar, J. Lumin., **166**, 167 (2015).
- [13] M. Dong, P. Zhou, C. Jiang, B. Cheng, J. Yu, Chem. Phys. Lett. 668, 1 (2017).
- [14] I. Devadoss, S. Muthukumaran, PhysicaE., **72**, 111 (2015).
- [15] M.B. Mohamed, Z.K. Heiba, N.G. Imam, J. Mol. Struct. 1163, 442 (2018).
- [16] R.N. Bhargava, J. Lumin., **70(1-6)**, 85 (1996).
- [17] Ubale S & Kulkarni D K., Bull Mater Sci, 2005, 28(1), 43.
- [18] B Elidrissi, M Addou, M Regragui, A Bougrine, A Kachouane, JC Bernede, Mater Chem. Phys., 2001, 68, 175.
- [19] P. Krishnamurthi and E. Murugan, Journal of Current Charmaceutical Research., **11(1)**, 38-42(2013).
- [20] J. Millman "Microelectronics" Murray Hill, Book Company Kogakusha, 1979, 642, P.172.
- [21] E. R. Shaaban, I. Kansal, S. Mohamed, J. Ferreira, Physica B: Condensed Matter., **404**, 3571(2009).
- [22] E. R. Shaaban, J. Alloys Compd. 563 (2013) 274.
- [23] J. Zhang, L. Feng, W. Cai, J. Zheng, Y. Cai, B. Li, L. Wu, Y. Shao, Thin Solid Films., **414**, 113–118.
- [24] A. Goktas, F. Aslan, I. H. Mutlu, J Mater Sci: Mater Electron ., **23**, 605–611(2012).
- [25] A. M. El Sayed, G. Said, S. Taha, A. Ibrahim, F. Yakuphanoglu, Superlattices Microstruct., **62**, 47–58(2013).

- [26] R. Swanepoel, *Journal of Physics E: Scientific Instruments*, **17**, 896- 903(1984).
- [27] E. R. Shaaban, Y. A. M. Ismail, H. S. Hassam, *Journal Non-crystalline solids.*, 376, 61-67 (3013).
- [28] R. Swanepoel, *Journal of Physics E: Scientific Instruments.*, **16**, 1214- 1222(1983).
- [29] Moss, T. S. "Optical Properties of Semi-Conductors (Butterworths Scientific, London, 1959)."
- [30] S. Kose, F. Atay, V. Bilgin, I. Akyuz, E. Ketenci, *Applied surface science.*, **256**, 4299-4303(2010).
- [31] M. Emam-Ismail.M. El-Hagary, E. R. Shaaban, A. M. Al Hedeib, *Journal of Alloys and Compounds* 532, 16-24 (2012)
- [32] R. Vahalová, L. Tichý, M. Vlček, H. Tichá, *physica status solidi (a)* 181(2000)199–209.
- [33] M. Mohamed, E. Shaaban, M.N. Abd-el Salam, A. Abdel-Latif, S.A. Mahmoud, M. Abdel-Rahim, *Optik*, **178**, 1302-1312(2019).
- [34] J. Tauc, *Amorphous and Liquid Semiconductor* (New York: Plenum) 1974, Ch4 159-214.
- [35] N. H. Hong, J. Sakai, N. T. Huong, Poirot N, Ruyter. *Phys Rev B.*, **72(4)**, 045336(2005).
- [36] ELS Yousef, A. Aladwy, N. El Koshkhany, E. R. Shaaban, *Journal Physics and Chemistry of solids.* 67(8), 1649-1655 (2006).
- [37] S. Ramachandran, J. Narayan, J. Prater. *Appl Phys Lett.*, **88(24)**, 242503(2006).
- [38] S. Koshihara, A. Oiwa, M. Hirasawa, S. Katsumoto, Y. Iye, C. Urano, et al. *Phys Rev Lett.*, **78(24)**, 4617-20(1997).
- [39] J. Singh, N. Verma.. *J Supercond Novel Magn.*, **27(10)**, 2371-7(2014).
- [40] T. R. Kumar, P. Prabukanthan, G. Harichandran, J. Theerthagiri, S. Chandrasekaran, J. Madhavan.. *Ionics.* **23(9)**, 2497-507(2017).
- [41] S. Kose, F. Atay, V. Bilgin, I. Akyuz, E. Ketenci, *Applied surface science.*, **256** (2010) 4299-4303.
- [42] E. R. Shaaban, M. S. Abd El-Sadek, M.El-Hagary, I. S.Yahia, *Physica Scripta* 86 (1), 015702 (2012)
- [43] C. Kittel, *Introduction to Solid State Physics*, 7th ed. (John Wiley & Sons Inc., Singapore, 1996), p. 308.
- [44] E. R. Shaaban, *Philosophical Magazine.*, **88(5)** 781(2008).
- [45] El-Nahass, M. M., H. S. Soliman, and A. A. Hendi. Sh. El-Gamdy, *Australian Journal of Basic and Applied Sciences.*, **5.6**, 145-156(2011).
- [46] H. Ticha, L. Tichy, *Journal of Optoelectronics and Advanced Materials.*, **4**, 381-386(2002).
- [47] K. Tanaka, *Optical properties and photoinduced changes in amorphous As-S films*, *Thin Solid Films.*, **66**, 271-279(1980).
- [48] L. Liu, T. Cheng, K. Nagasaka, H. Tong, G. Qin, T. Suzuki, and Y. Ohishi, *Opt. Lett.*, **41**, 392-395(2016).
- [49] E.R. Shaaban, M. Abdel-Rahman, El Sayed Yousef, M.T. Dessouky. *Thin Solid Films.*, **515**, 3810(2007).
- [50] N. F. Mott, E. A. Davis & R. A. Street · *Philosophical Magazine.*, **32 (5)**, 961-996 (1975).